Free Radical Biology and Medicine 67 (2014) 211–220

Contents lists available at ScienceDirect

Free Radical Biology and Medicine

journal homepage: www.elsevier.com/locate/freeradbiomed

Original Contributions

Contribution of endogenously produced reactive oxygen species to the activation of podocyte NLRP3 inflammasomes in hyperhomocysteinemia

Justine M. Abais [a], Min Xia [a], Guangbi Li [a], Todd W.B. Gehr [b], Krishna M. Boini [a], Pin-Lan Li [a,*]

[a] Department of Pharmacology and Toxicology, Virginia Commonwealth University School of Medicine, Richmond, VA 23298, USA
[b] Department of Internal Medicine, Virginia Commonwealth University School of Medicine, Richmond, VA 23298, USA

ARTICLE INFO

Article history:
Received 10 May 2013
Received in revised form
2 October 2013
Accepted 8 October 2013
Available online 16 October 2013

Keywords:
Homocysteine
NLRP3 inflammasome
Redox signaling
Glomerular sclerosis
Free radicals

ABSTRACT

Hyperhomocysteinemia (hHcys) is an important pathogenic factor contributing to the progression of end-stage renal disease. Recent studies have demonstrated the implication of nicotinamide adenine dinucleotide phosphate oxidase-mediated NLRP3 inflammasome activation in the development of podocyte injury and glomerular sclerosis during hHcys. However, it remains unknown which reactive oxygen species (ROS) are responsible for this activation of NLRP3 inflammasomes and how such action of ROS is controlled. This study tested the contribution of common endogenous ROS including superoxide ($O_2^{\bullet -}$), hydrogen peroxide (H_2O_2), peroxynitrite ($ONOO^-$), and hydroxyl radical ($^{\bullet}OH$) to the activation of NLRP3 inflammasomes in mouse podocytes and glomeruli. In vitro, confocal microscopy and size-exclusion chromatography demonstrated that dismutation of $O_2^{\bullet -}$ by 4-hydroxy-2,2,6,6-tetramethylpiperidine 1-oxyl (Tempol) and decomposition of H_2O_2 by catalase prevented Hcys-induced aggregation of NLRP3 inflammasome proteins and inhibited Hcys-induced caspase-1 activation and IL-1β production in mouse podocytes. However, scavenging of $ONOO^-$ or $^{\bullet}OH$ had no significant effect on either Hcys-induced NLRP3 inflammasome formation or activation. In vivo, scavenging of $O_2^{\bullet -}$ by Tempol and removal of H_2O_2 by catalase substantially inhibited NLRP3 inflammasome formation and activation in glomeruli of hHcys mice as shown by reduced colocalization of NLRP3 with ASC or caspase-1 and inhibition of caspase-1 activation and IL-1β production. Furthermore, Tempol and catalase significantly attenuated hHcys-induced glomerular injury. In conclusion, endogenously produced $O_2^{\bullet -}$ and H_2O_2 primarily contribute to NLRP3 inflammasome formation and activation in mouse glomeruli resulting in glomerular injury or consequent sclerosis during hHcys.

Elevated levels of plasma homocysteine, namely, hyperhomocysteinemia (hHcys), have been extensively studied as a deleterious cause of a wide range of chronic pathological conditions, including vascular dysfunction, neurological diseases, metabolic disorders, the development of cancer, and many complications associated with aging [1–7]. Emerging evidence demonstrates a crucial role of hHcys in the progression of end-stage renal disease (ESRD) associated with various systemic syndromes or local kidney diseases such as hypertension, diabetic mellitus, and chronic kidney diseases. It has been shown to be a major pathogenic factor contributing to cardiovascular complications from ESRD [8,9]. Mechanistically, previous studies have shown that hHcys-induced glomerular sclerosis and ultimate ESRD involve NMDA receptor activation and occur in a nicotinamide adenine dinucleotide phosphate (NADPH) oxidase-dependent manner, which depends upon the activation of the small GTPase Rac1 and guanine nucleotide exchange factor Vav2 [10–12]. Most recently, Nod-like receptor protein 3 (NLRP3) inflammasome-mediated caspase-1 activation and IL-1β production were found to be necessary for hHcys-induced podocyte and glomerular dysfunction, where inhibition of NLRP3 inflammasomes either by apoptosis-associated speck-like protein (ASC) gene silencing or by pharmacological inhibition of caspase-1 attenuated hHcys-induced injury [13]. This NLRP3 inflammasome activation is associated with NADPH oxidase activity and production of superoxide ($O_2^{\bullet -}$) [14]. NADPH oxidase and the reactive oxygen species (ROS) derived from its activity have been well correlated with many chronic diseases [15]. However, with many other ROS potentially involved, it remains unknown whether NADPH oxidase-derived $O_2^{\bullet -}$ itself or perhaps other species contribute to hHcys-induced inflammasome activation in podocytes.

It has been reported that the NLRP3 inflammasome, an inflammatory machinery that when stimulated results in IL-1β maturation and triggers the early innate immunity cascade to initiate an

* Corresponding author. Fax: +1 804 828 4794.
E-mail address: pli@vcu.edu (P.-L. Li).

0891-5849/$ - see front matter © 2013 Elsevier Inc. All rights reserved.
http://dx.doi.org/10.1016/j.freeradbiomed.2013.10.009

immune response, comprises three major proteins—NLRP3, considered to be the sensory component; the adaptor protein ASC; and the effector caspase-1. Deficiencies in this multiprotein complex have been associated with autoimmune disorders such as familial Mediterranean fever and Muckle-Wells syndrome, but aberrant NLRP3 inflammasome activation has extended to many traditionally considered noninflammatory disorders, including diabetes, obesity, silicosis, liver toxicity, and vascular and kidney diseases [16–24]. The mechanism of how the NLRP3 inflammasome becomes activated in response to diverse endogenous and exogenous danger signals remains largely obscure. With the attempt of many studies to reach a clearer understanding, multiple pathways of inflammasome activation have been proposed. It has been indicated that after a "priming signal" resulting in the expression and intracellular accumulation of pro-IL-1β, there are three potential pathways that lead to the formation or activation of NLRP3 inflammasomes to trigger proteolytic cleavage of pro-IL-1β to the mature and secreted form [19,25–27]. One pathway suggests that K^+ efflux and low intracellular K^+ concentration resulting from toxin or ATP activation of the P2X7 receptor facilitates NLRP3 inflammasome assembly, whereas another suggests that frustrated or incomplete phagocytosis of large particulate signals causes lysosomal rupture, releasing cathepsin B, which promotes NLRP3 inflammasome activation in an undefined mechanism. Much evidence demonstrates that many inflammasome stimulators are also known to produce ROS, and the ROS model of inflammasome activation proposes NLRP3 to be a general sensor for changes in local and intracellular oxidative stress, allowing it to become activated in response to a diverse range of stimuli [19,25–27].

Although homocysteine (Hcys)-induced ROS production in podocytes has been documented, it remains unknown how this Hcys-induced ROS production is involved in activation of NLRP3 inflammasomes in podocytes and ultimate glomerular injury. We have previously shown that inhibition of NADPH oxidase prevents Hcys-induced podocyte dysfunction and more recently confirmed that inhibition of NADPH oxidase and the downstream production of $O_2^{\bullet -}$ abrogates NLRP3 inflammasome formation and activation [14,28]. However, it is poorly understood which species of ROS is responsible for NLRP3 inflammasome activation and how ROS lead to the formation or activation of this inflammasome. In this regard, recent studies have indicated that ROS may serve as important signaling messengers and that $O_2^{\bullet -}$ and hydrogen peroxide (H_2O_2) are common ROS that may act as second messengers to activate inflammasomes within podocytes. Hence, this study seeks to dissect the potential role of these endogenously produced ROS in Hcys-induced NLRP3 inflammasome activation and to determine which ROS are required for glomerular injury associated with such activation of NLRP3 inflammasomes.

Materials and methods

Cell culture

Kindly provided by Dr. Paul E. Klotman (Division of Nephrology, Department of Medicine, Mount Sinai School of Medicine, New York, NY, USA), a conditionally immortalized mouse podocyte cell line was cultured undifferentiated with 10 U/ml recombinant mouse interferon-γ at 33 °C on collagen I-coated flasks in RPMI 1640 medium containing 10% fetal bovine serum, 100 U/ml penicillin, and 100 mg/ml streptomycin. Passaged podocytes were allowed to differentiate at 37 °C for 10–14 days in the absence of interferon-γ before being ready for use in experiments. L-Hcys, the pathogenic form of Hcys, was added to cultured cells at a concentration of 40 μM for 24 h, the optimal treatment dose and time selected based on previous studies [13]. ROS scavengers were used at the following doses: 4-hydroxy-2,2,6,6-tetramethylpiperidine 1-oxyl (Tempol), 100 μM; catalase, 50 U/ml; tetramethylthiourea (TMTU), 100 μM; manganese(III) tetrakis(1-methyl-4-pyridyl) porphyrin (MnTMPyP), 25 μM; polyethylene glycol–superoxide dismutase (PEG–SOD), 50 U/ml; and ebselen, 10 μM.

Animals

Eight-week-old male C57BL/6J mice (The Jackson Laboratory, Bar Harbor, ME, USA) were uninephrectomized, an accepted method of accelerating renal injury, as described previously [14,29,30], and allowed 1 week for surgery recovery. For 4 weeks, mice received vehicle, Tempol, or catalase treatment and were fed either a normal diet or a folate-free (FF) diet to induce hHcys. Folates are a cofactor required for the breakdown of Hcys, and restricting folate consumption in the diet prevents the remethylation of Hcys back to methionine, causing elevated levels of plasma Hcys [11,31]. Tempol (3 mM; Sigma, St. Louis, MO, USA) was administered to the mice through the drinking water, whereas catalase (Sigma) was injected intraperitoneally at a dose of 5000 U/kg/day [32,33]. At the end of the 4-week treatment, before blood collection, sacrificing, and harvesting of kidney tissue, urine samples were collected as mice were placed in metabolic cages for 24 h. All animal procedures and protocols were approved by the Institutional Animal Care and Use Committee of Virginia Commonwealth University.

Confocal microscopic detection of inflammasome proteins

The colocalization of inflammasome proteins was observed through indirect immunofluorescent staining of both treated podocytes and frozen mouse kidney sections. In vitro, podocytes were cultured in eight-well chambers and pretreated for 1 h with various ROS scavengers before incubation with 40 μM L-Hcys for 24 h. Cells were fixed in 200 μl of 4% paraformaldehyde for 15 min, washed with phosphate-buffered saline (PBS) before blocking with 1% bovine serum albumin in PBS, and incubated with primary antibodies overnight at 4 °C. The primary antibodies and concentrations used were as follows: goat anti-NLRP3, 1:100 (Abcam, Cambridge, MA, USA), with rabbit anti-ASC, 1:100 (Santa Cruz Biotechnology, Dallas, TX, USA), or goat anti-NLRP3 with rabbit anti-caspase-1, 1:100 (Santa Cruz Biotechnology). As for immunofluorescent staining in the mouse glomeruli, frozen slides were fixed in acetone and blocked with 3% donkey serum before overnight incubation at 4 °C with goat anti-NLRP3 (1:50) and rabbit anti-ASC (1:50) or goat anti-NLRP3 and rabbit anti-caspase-1 (1:50). NLRP3 or caspase-1 colocalization was also measured against podocyte markers podocin (1:50; Sigma) or desmin (1:50; BD Biosciences, San Jose, CA, USA), as well as glomerular endothelial and mesangial cell markers VE-cadherin (1:50; Abcam) and α-SMA (1:50; Abcam), to validate the in vivo formation of inflammasomes in podocytes of the mouse glomeruli. Double immunofluorescent staining was completed in both cultured podocytes and frozen slides by Alexa-488 or Alexa-555-labeled secondary antibody (1:200 podocytes, 1:50 frozen slides; Invitrogen, Carlsbad, CA, USA) incubation for 1 h at room temperature. After being washed, slides were mounted with Vectashield mounting medium containing DAPI (Vector Laboratories, Burlingame, CA, USA) and colocalization was observed using a confocal laser scanning microscope (Fluoview FV1000; Olympus, Tokyo, Japan). As described in our previous studies, Image Pro Plus 6.0 software (Media Cybernetics, Bethesda, MD, USA) was employed to analyze colocalization, expressed as the Pearson correlation coefficient [13,14,34].

Size-exclusion chromatography (SEC) and Western blotting

SEC was performed as described previously [14,35], where cultured podocytes were treated with various ROS scavengers in the presence of Hcys, as mentioned above. Briefly, the homogenate from podocytes was prepared using the following protein extraction buffer: 20 mM 4-(2-hydroxyethyl)-1-piperazineethanesulfonic acid–KOH (pH 7.5), 10 mM KCl, 1.5 mM Na-EDTA, 1 mM Na-EGTA, and 1 × protease inhibitor cocktail (Roche Applied Science, Indianapolis, IN, USA). Samples were centrifuged at 14,000 rpm for 10 min at 4 °C to remove debris, the supernatant was filtered through a 0.45-μm cellulose acetate centrifuge tube filter, and all samples were normalized by measuring their protein concentration. A total of 1 mg protein for all samples was run on a Superose 6 10/300 GL column using an ÄKTAprime Plus fast-protein liquid chromatography system (GE Healthscience, Uppsala, Sweden). Fractions of 600 μl were collected and protein was precipitated and analyzed by SDS–polyacrylamide gel electrophoresis (SDS–PAGE). Loading buffer (5 ×) was added to the precipitated samples, boiled, and run on a 12% gel, and protein was transferred to a polyvinylidene difluoride membrane at 100 V for 1 h. After blocking, the membrane was probed with anti-ASC (1:1000; Enzo, Farmingdale, NY, USA) overnight at 4 °C, followed by incubation with horseradish peroxidase-labeled IgG (1:5000). The chemiluminescent bands were detected and visualized on Kodak Omat X-ray film, using the ImageJ software (NIH, Bethesda, MD, USA) to analyze band density.

Caspase-1 activity, IL-1β production, and urinary protein measurements

Caspase-1 activity was measured by a colorimetric assay made commercially available by Biovision (Mountain View, CA, USA), and IL-1β production was measured through an enzyme-linked immunosorbent assay (R&D Systems, Minneapolis, MN, USA) and used following the manufacturer's instructions. Total urinary protein excretion was determined spectrophotometrically using the Bradford assay (Sigma).

Analysis of $O_2^{\bullet -}$ production

NADPH oxidase-dependent $O_2^{\bullet -}$ production was determined in protein extracted from renal cortical tissue using a sucrose buffer, which was then resuspended in a modified Krebs–Hepes buffer containing deferoximine (100 μM; Sigma) and diethyldithiocarbamate (5 μM; Sigma). NADPH substrate (1 mM) was added to 20 μg protein, and each sample was tested in both the presence and the absence of SOD (200 U/ml; Sigma) to assess $O_2^{\bullet -}$ specificity. The $O_2^{\bullet -}$-specific spin trapping compound 1-hydroxy-3-methoxycarbonyl-2,2,5,5-tetramethylpyrrolidine (CMH; 1 mM; Noxygen, Elzach, Germany) was included in the sample before analysis in an ESR spectrometer (Magnettech Ltd, Berlin, Germany) using the following settings: biofield, 3360; field sweep, 60 G; microwave frequency, 8 GHz; microwave power, 20 mW; modulation amplitude, 3 G; 4096 points of resolution; receiver gain, 20 for tissue. The SOD-specific signal was calculated by subtracting the signal obtained in the presence of SOD from the total CMH signal without SOD, with all values being expressed relative to control podocytes [14,36,37].

Glomerular morphological examination

Fixed kidney tissues were paraffin embedded and stained with periodic acid–Schiff (PAS). Using a light microscope, glomerular morphology was observed and assessed semiquantitatively by counting 50 glomeruli per slide and scoring each as 0, 1, 2, 3, or 4. These values were respectively assigned according to the severity of sclerotic changes (0, <25, 25–50, 51–75, or >75% sclerosis of the glomerulus). The Glomerular Damage Index comprised the average of these scores and was calculated according to the following formula: $((N_1 \times 1) + (N_2 \times 2) + (N_3 \times 3) + (N_4 \times 4))/n$, where N_1, N_2, N_3, and N_4 respectively represent the numbers of glomeruli with scores of 1, 2, 3, and 4, and n represents the total number of scored glomeruli [14,36].

Real-time reverse transcription polymerase chain reaction (PCR)

Total RNA was isolated from podocytes, reverse transcribed to cDNA, and subject to PCR amplification according to the procedures described previously [38]. Primers were synthesized by Operon (Huntsville, AL, USA) with the following sequences: Nox1, sense AATGCCCAGGATCGAGGT, antisense GATGGAAGCAAAGGGAGTGA; Nox2, sense TGGCACATCGATCCCTCACTGAAA, antisense GGTCACTGCATCTAAGGCAACCT; Nox4, sense GAAGGGGTTAAACACCTCTGC, antisense ATGCTCTGCTTAAACACAATCCT.

Analysis of plasma Hcys by high-performance liquid chromatography (HPLC)

Total Hcys levels were measured in the plasma of mice according to detailed methods described previously [36].

Statistical analysis

Data are expressed as the mean ± SEM, and significance was determined using one-way ANOVA followed by the Student–Newman–Keuls post hoc test. The χ^2 test was used to determine significance of ratio and percentage data. $P < 0.05$ was considered statistically significant.

Results

Reduction of intracellular $O_2^{\bullet -}$ and H_2O_2 levels prevented Hcys-induced NLRP3 inflammasome formation in podocytes

Using the $O_2^{\bullet -}$ dismutase mimetic Tempol, H_2O_2 decomposer catalase, or $^{\bullet}OH$ scavenger TMTU, we tested whether Hcys-induced inflammasome formation and activation can be altered. By confocal microscopy analysis, we demonstrated that Hcys induced colocalization (yellow spots) of inflammasome molecules (NLRP3 (green) vs ASC or caspase-1 (red)) in podocytes, compared to control cells, suggesting increased formation of NLRP3 inflammasomes (Fig. 1A). However, prior treatment of podocytes with Tempol or catalase blocked Hcys-induced colocalization of NLRP3 with ASC or caspase-1. In contrast, TMTU did not block Hcys-induced inflammasome formation, suggesting that $O_2^{\bullet -}$ and H_2O_2, but not $^{\bullet}OH$, is involved in Hcys-induced inflammasome formation in podocytes. The colocalization coefficient analyses were summarized and are shown in Fig. 1B. These effects are thought to originate from ROS derived by specific Nox2 activation and, furthermore, this Hcys-induced Nox2 mRNA upregulation was unaffected by $O_2^{\bullet -}$ scavenging, suggesting that the subsequent effects of scavenging these ROS are due to events occurring downstream of NADPH oxidase activation (Supplementary Fig. 1).

To further confirm inflammasome formation in response to elevated Hcys, size-exclusion chromatography was employed and further provided evidence that Tempol or catalase treatment prevented Hcys-induced inflammasome formation, as shown by the inhibited shift of ASC proteins into higher molecular weight fractions (Fig. 2B). These fractions are compared to a standard protein size marker in Fig. 2A, a representative chromatogram showing proteins that are part of the inflammasome complex

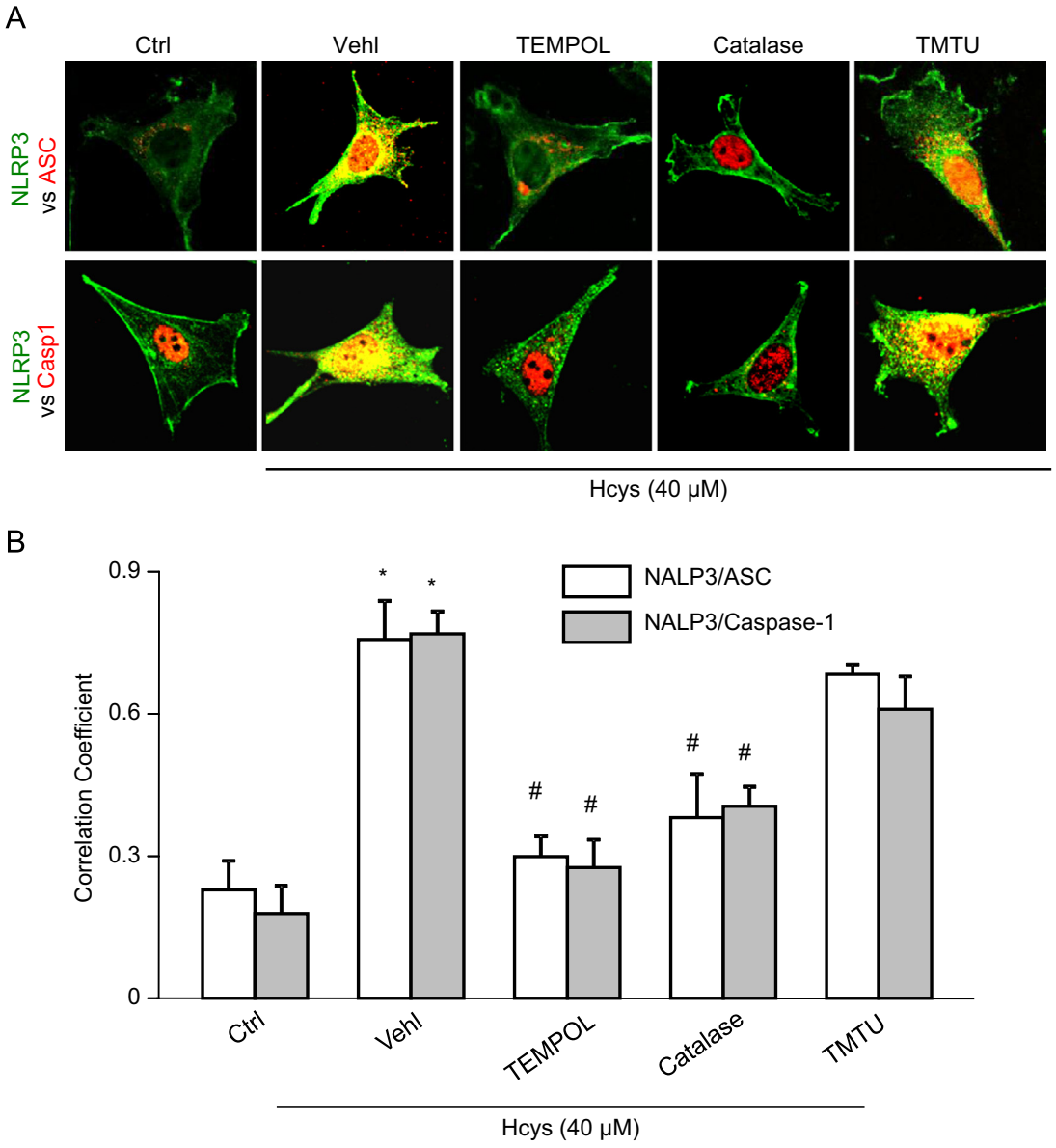

Fig. 1. Tempol and catalase attenuate Hcys-induced inflammasome formation in podocytes. (A) Confocal images representing the colocalization of NLRP3 (green) with ASC or caspase-1 (red) in cultured podocytes. (B) Summarized data showing the fold change in PCC for the colocalization of NLRP3 with ASC and NLRP3 with caspase-1 ($n = 4$). Ctrl, control; Vehl, vehicle; TMTU, tetramethylthiourea; PCC, Pearson coefficient correlation. $^{*}P < 0.05$ vs control; $\#P < 0.05$ vs Hcys. (For interpretation of the references to color in this figure legend, the reader is referred to the web version of this article.)

eluted within fractions 3–7 and were analyzed by SDS–PAGE. The intensities of bands were quantified and are summarized in Fig. 2C, showing that scavenging of $O_2^{\bullet -}$ and H_2O_2, but not $^{\bullet}OH$, was able to inhibit inflammasome formation in podocytes treated with Hcys.

Tempol and catalase, but not TMTU or ebselen, blocked activation of NLRP3 inflammasomes in podocytes

Aside from measures of NLRP3 inflammasome formation, previous studies have indicated that caspase-1 activation and IL-1β production reflect the activation of NLRP3 inflammasomes [1,40]. In the present study, we tested whether Tempol and catalase abolish Hcys-induced NLRP3 inflammasome activation. As shown in Fig. 3, Hcys treatment significantly increased caspase-1 activity and IL-1β production compared to control cells. However, pretreatment of podocytes with either Tempol or catalase significantly attenuated Hcys-induced increases in caspase-1 activity and IL-1β secretion, indicating that $O_2^{\bullet -}$ and H_2O_2 are necessary for the functionality of inflammasomes in response to Hcys. In addition we also tested the role of another SOD mimetic, MnTMPyP, as well as cell-permeable PEG–SOD in podocytes with or without Hcys stimulation. We found that pretreatment with either MnTMPyP or PEG–SOD significantly attenuated the Hcys-induced caspase-1 activity and IL-1β production (Supplementary Fig. 2). We demonstrated that scavenging of $^{\bullet}OH$ by TMTU or the use of ebselen (a putative $ONOO^-$ scavenger) did not have effects on Hcys-induced NLRP3 inflammasome formation and activation in podocytes. In the following in vivo studies, therefore, six groups of experiments are presented that include mice on the normal or FF diet with or without Tempol and catalase.

Tempol and catalase prevented NLRP3 inflammasome formation and activation in the glomeruli of hyperhomocysteinemic mice

To further determine whether $O_2^{\bullet -}$ and H_2O_2 are implicated in inflammasome formation and activation in vivo, C57BL/6J wild-type

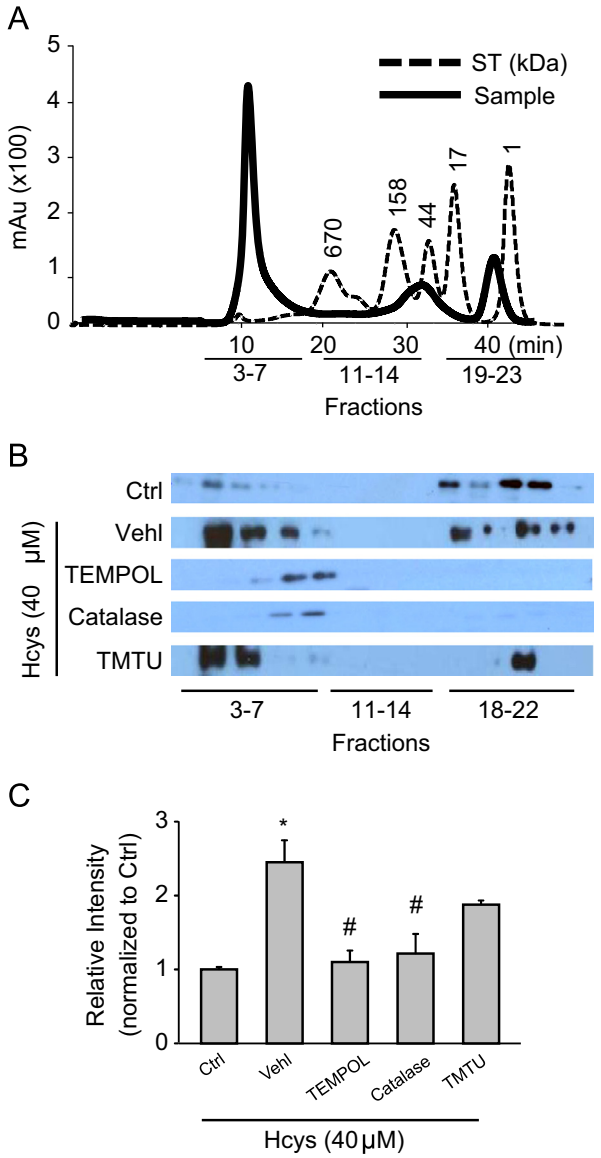

Fig. 2. Size-exclusion chromatography demonstrates inhibition of Hcys-induced ASC protein redistribution after $O_2^{\bullet -}$ and H_2O_2 scavenging. (A) Representative chromatograms illustrating the elution profiles of proteins from both a standard and a podocyte sample taken from an absorbance of 280 nm. Elution of a gel filtration standard allowed for the determination of the molecular mass of the samples. (B) Selected protein fractions were analyzed by Western blot, probed with an anti-ASC antibody. (C) Summarized data determined from the ASC band intensities of the inflammasome complex fractions (3–7) ($n = 4$–6). Ctrl, control; Vehl, vehicle; TMTU, tetramethylthiourea. $^*P < 0.05$ vs control; $\#P < 0.05$ vs Hcys.

mice were treated with Tempol or catalase and fed a normal diet (ND) or FF diet for 4 weeks. HPLC analysis revealed that FF diet treatment significantly increased the plasma total Hcys levels in uninephrectomized C57BL/6J mice compared with ND-fed mice. Neither uninephrectomy nor the treatment with Tempol or catalase altered the Hcys levels on either diet (Supplementary Fig. 3). As shown in Fig. 4, the glomeruli of mice maintained on the FF diet had increased colocalization of NLRP3 with ASC or NLRP3 with caspase-1 compared to ND-fed mice, suggesting the formation of NLRP3 inflammasomes in glomeruli of hyperhomocysteinemic mice. hHcys, known to cause podocyte injury, significantly decreased the amount of podocin staining in the glomeruli, thus resulting in minimal colocalization with inflammasome protein NLRP3 (Fig. 5). However, the formation of hHcys-induced NLRP3 inflammasomes mainly occurred in injured podocytes within glomeruli, evidenced by the increased colocalization of NLRP3 with the podocyte damage marker desmin (Fig. 5). This colocalization of NLRP3 was not evident with either VE-cadherin or α-SMA, respective markers of glomerular endothelial and mesangial cells (Supplementary Fig. 4). Correspondingly, caspase-1 activity and IL-1β production were significantly enhanced in hyperhomocysteinemic mice compared to normal diet-fed mice, further confirming NLRP3 inflammasome activation (Fig. 6A and B). Concurrent with this inflammasome activation, SOD-sensitive $O_2^{\bullet -}$ production was 2.1-fold greater in mice fed the FF diet than in those on the ND (Fig. 6C). All of these hHcys-induced effects on parameters of inflammasome formation and activation were abolished by administration of either the SOD mimetic Tempol or the H_2O_2 decomposer catalase. Taken together, these data suggest that both $O_2^{\bullet -}$ and H_2O_2 play pivotal roles in hHcys-induced NLRP3 inflammasome formation and activation in glomeruli of hyperhomocysteinemic mice.

In vivo Tempol and catalase administration protected mouse glomeruli from hHcys-induced dysfunction and injury

As shown in Fig. 7, FF diet-induced hHcys resulted in significantly elevated urinary protein excretion as well as marked pathological changes in glomerular morphology, compared to mice on the ND. However, the hHcys-induced proteinuria and glomerular injury were not evident in hyperhomocysteinemic mice treated with Tempol or catalase. Dismutation of $O_2^{\bullet -}$ and decomposition of H_2O_2 was able to prevent hHcys-induced renal dysfunction and glomerular damage, signifying the importance of $O_2^{\bullet -}$ and H_2O_2 in the mechanism of hHcys-induced injury.

Discussion

The goal of this study was to dissect which endogenously produced ROS in response to increased Hcys in podocytes in vitro and in vivo contribute to hHcys-induced NLRP3 inflammasome formation and activation. Studies using cultured podocytes revealed that reduction of intracellular $O_2^{\bullet -}$ and H_2O_2 levels attenuated Hcys-induced NLRP3 inflammasome formation and suppressed downstream caspase-1 activation and IL-1β production. In vivo, dismutation of $O_2^{\bullet -}$ and decomposition of H_2O_2 in hyperhomocysteinemic mice not only prevented NLRP3 inflammasome formation in glomeruli, but also protected mice with hHcys from renal dysfunction and glomerular sclerosis. To our knowledge, this study is the first effort to dissect endogenously produced ROS in NLRP3 inflammasome activation in podocytes and glomeruli during exposure to high Hcys levels or hHcys.

There is accumulating evidence indicating that hHcys contributes to the development of a number of degenerative or sclerotic diseases including coronary artery disease, multiple sclerosis, Parkinson's disease, and many complications associated with aging in general, such as osteoporosis and cognitive decline [4,39–43]. Elevated levels of this methionine amino acid intermediate have also been considered to be an independent risk factor for chronic renal disease, promoting glomerular dysfunction and end-stage renal disease. Interestingly, renal dysfunction may further elevate plasma Hcys due to impaired renal excretory function, resulting in a so-called vicious cycle and ultimately the development of glomerular sclerosis [44]. In the present study, mice fed a FF diet for 4 weeks indeed exhibited elevated plasma Hcys, significant glomerular structural deterioration, and hindered glomerular function such as proteinuria. We have recently linked these deleterious effects of hHcys to NLRP3 inflammasome formation and activation, in that inhibiting the assembly of this multiprotein

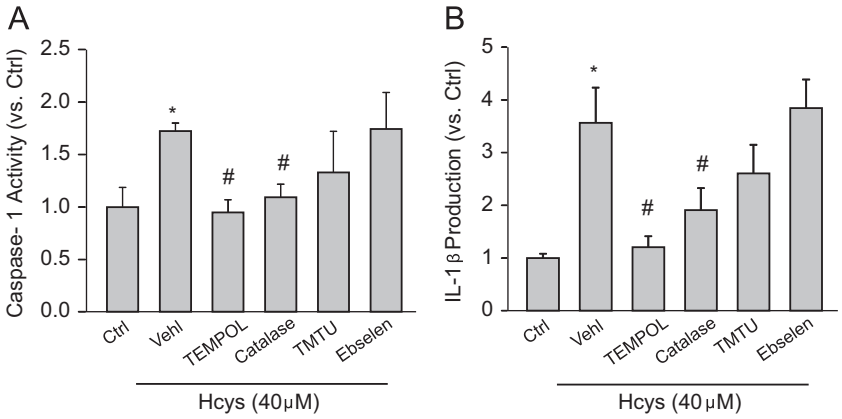

Fig. 3. Effects of ROS scavenging on caspase-1 activity and IL-1β secretion in the presence of Hcys. (A) Caspase-1 activity, shown as folds versus Ctrl, measured in podocytes treated with Hcys in the presence of various ROS scavengers ($n = 6–8$). (B) IL-1β production measured in the supernatant of podocytes treated with Hcys in the presence of various ROS scavengers ($n = 6–8$). Ctrl, control; Vehl, vehicle; TMTU, tetramethylthiourea. *$P < 0.05$ vs control; #$P < 0.05$ vs Hcys.

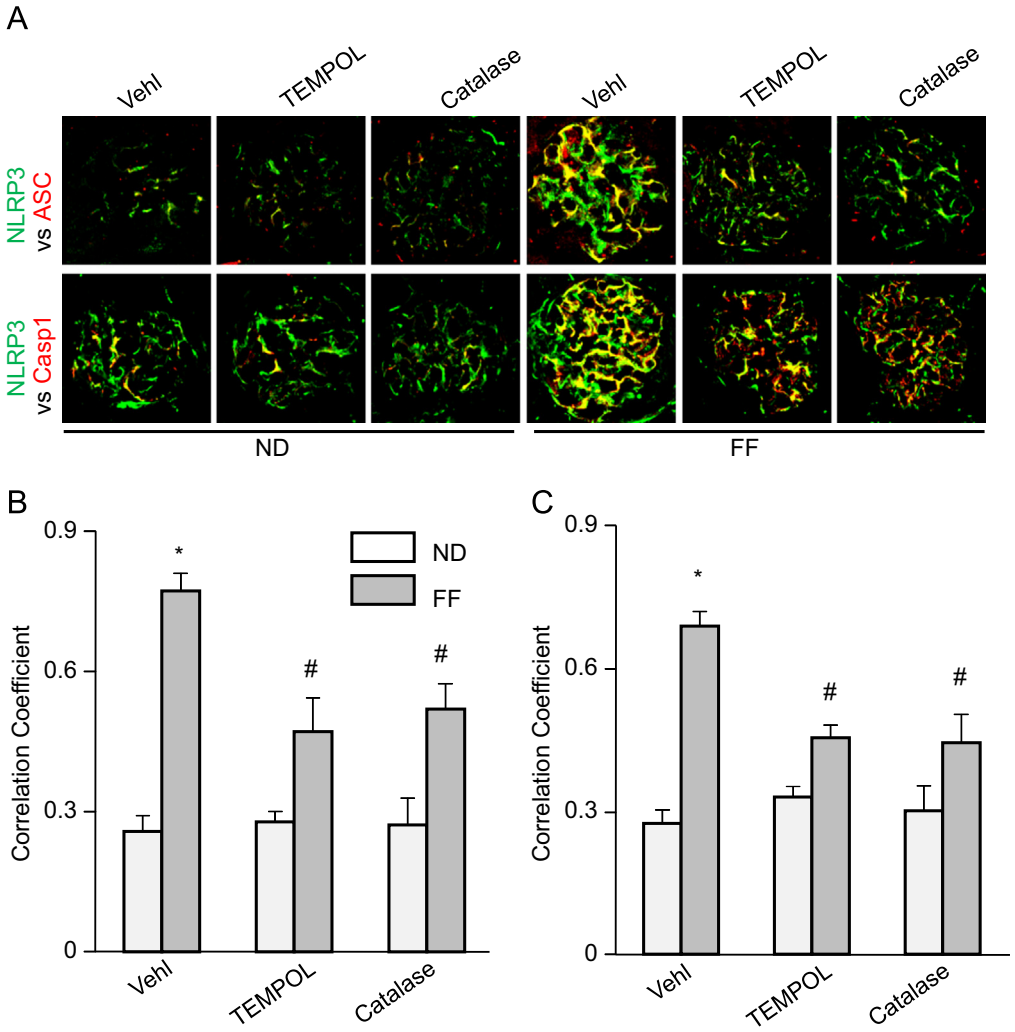

Fig. 4. In vivo effects of $O_2^{\bullet -}$ and H_2O_2 inhibition on hHcys-induced inflammasome formation in podocytes of hyperhomocysteinemic mice. (A) Colocalization of NLRP3 (green) with ASC or caspase-1 (red) in the mouse glomeruli of vehicle-, Tempol-, or catalase-treated mice fed a normal or FF diet. (B and C) Summarized data showing the correlation coefficients between NLRP3 with ASC or caspase-1 ($n = 6$). Casp1, caspase-1; Vehl, vehicle; ND, normal diet; FF, folate-free diet. *$P < 0.05$ vs Vehl on ND; #$P < 0.05$ vs Vehl on FF diet. (For interpretation of the references to color in this figure legend, the reader is referred to the web version of this article.)

complex prevented all these injurious effects of hHcys to the glomeruli [13]. Additional investigations revealed that this activation was dependent on NADPH oxidase-derived $O_2^{\bullet -}$, because both genetic and pharmacologic inhibition of NADPH oxidase expression or activity significantly reduced NLRP3 inflammasome formation and activation [14]. Although several models postulate as to how the NLRP3 inflammasome is activated in response to a diverse number of stimulators, many studies have accredited the activation of NLRP3 inflammasomes to the production of ROS [26], which was determined in this study.

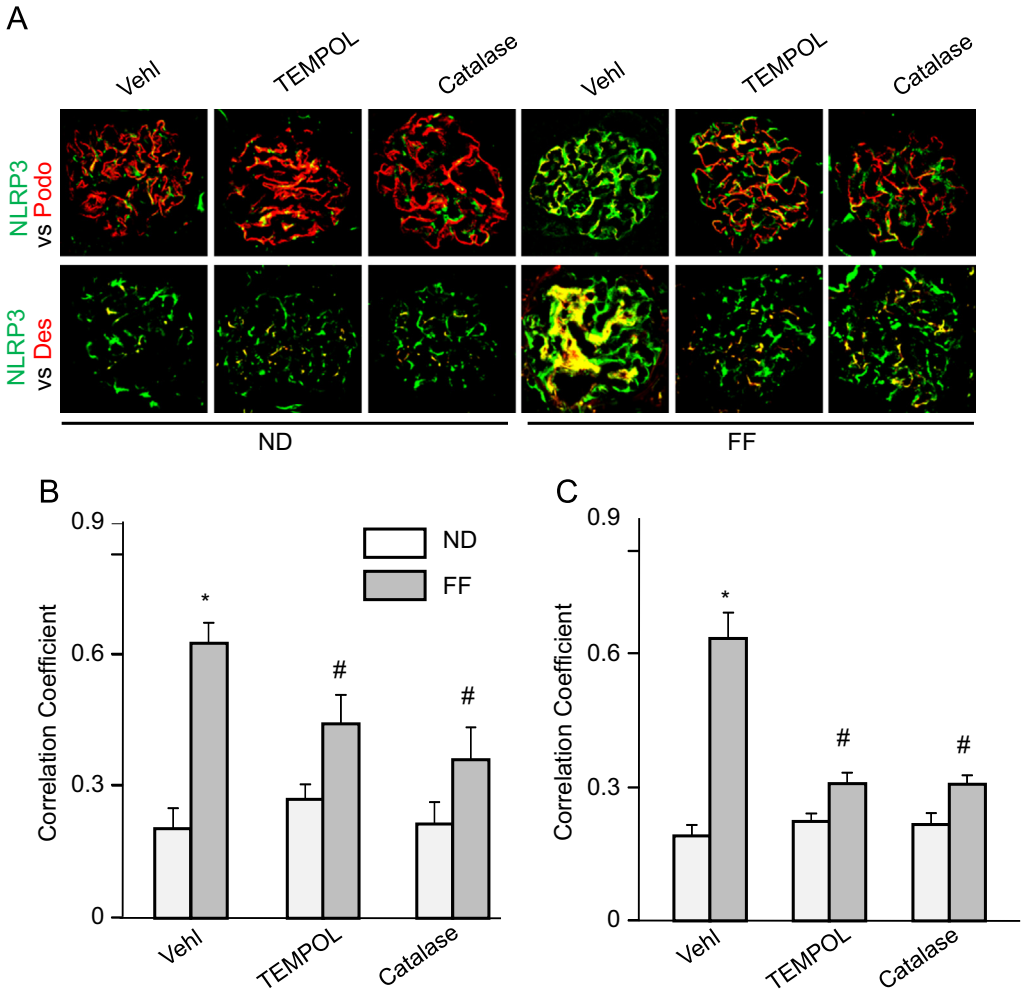

Fig. 5. hHcys-induced inflammasome formation occurs primarily in podocytes of hyperhomocysteinemic mouse glomeruli. (A) Colocalization of NLRP3 (green) with podocyte markers podocin or desmin (red) in the mouse glomeruli of vehicle-, Tempol-, or catalase-treated mice fed a normal or FF diet. (B and C) Summarized data showing the correlation coefficient between NLRP3 with podocin or desmin ($n = 6$). Podo, podocin; Des, desmin; Vehl, vehicle; ND, normal diet; FF, folate-free diet. *$P < 0.05$ vs Vehl on ND; #$P < 0.05$ vs Vehl on FF diet. (For interpretation of the references to color in this figure legend, the reader is referred to the web version of this article.)

Many studies provided increasing evidence for the central role of ROS in NLRP3 inflammasome activation [19,24,45,46]. Additional studies have demonstrated, through the use of either NADPH oxidase inhibitors or general ROS scavengers such as diphenylene iodonium and *N*-acetylcysteine, that IL-1β production in response to even more diverse stimuli could be prevented [47–50]. However, by using these general ROS scavengers, it remains largely unexplored as to exactly which species of ROS is being sensed and is indeed contributing to NLRP3 inflammasome activation. Aside from $O_2^{\bullet -}$, other species derived from NADPH oxidase include H_2O_2, peroxynitrite ($ONOO^-$), and $^{\bullet}OH$ [51]. A small subset of reports has attempted the use of ROS scavengers, but to our knowledge, the present study is the first to dissect these common endogenously produced ROS to elucidate their roles in hHcys-induced NLRP3 inflammasome activation.

Tempol, used for its antioxidant properties, has been widely demonstrated to have protective effects against many disease models, including diabetes, cardiovascular complications, heart failure, angiogenesis, ischemia–reperfusion injury, cancer, and glomerular injury [52–54]. Catalase is responsible for the enzymatic decomposition of H_2O_2 down to H_2O and O_2 [55,56], and TMTU has been used as a specific $^{\bullet}OH$ scavenger [54]. These pharmacologic tools enabled the dissection of the ROS participating in Hcys-induced NLRP3 inflammasome formation and activation. We demonstrated that in vitro dismutation of $O_2^{\bullet -}$ by Tempol or decomposition of H_2O_2 by catalase, but not scavenging of $^{\bullet}OH$ by TMTU or $ONOO^-$ by ebselen, prevented NLRP3 inflammasome formation as shown by inhibition of Hcys-induced colocalization of inflammasome proteins and by inhibition of Hcys-induced shift of ASC protein to higher molecular weight fractions termed the "inflammasome fractions." Accompanying these effects, treatment of podocytes with Tempol or catalase before Hcys also resulted in diminished caspase-1 activation and IL-1β production, indicating inhibition of inflammasome activation. Similarly, in vivo dismutation of $O_2^{\bullet -}$ produced NLRP3 inflammasome-inhibiting results parallel to those in vitro, and it furthermore displayed protective effects against hHcys-induced podocyte and glomerular injury, precluding sclerotic morphological changes and proteinuria. However, the use of Tempol is fairly limited in that its selectivity for $O_2^{\bullet -}$ is quite restricted due to a number of nonspecific targets, hence our use of PEG–SOD as well as an additional SOD mimetic, MnTMPyP, in in vitro experiments to further verify our results. But, similar to our findings in podocytes or glomeruli, a recent report provided evidence that scavenging of extracellular $O_2^{\bullet -}$ by the SOD mimetic Mn(III) tetrakis(*N*-ethylpyridinium-2-yl) porphyrin could prevent NLRP3 inflammasome activation in a model of hypoxia-induced pulmonary hypertension [57]. In addition, Zhou et al. [19] demonstrated the ability of exogenous H_2O_2 to directly activate NLRP3 inflammasomes to produce IL-1β. Taken together, these data suggest the

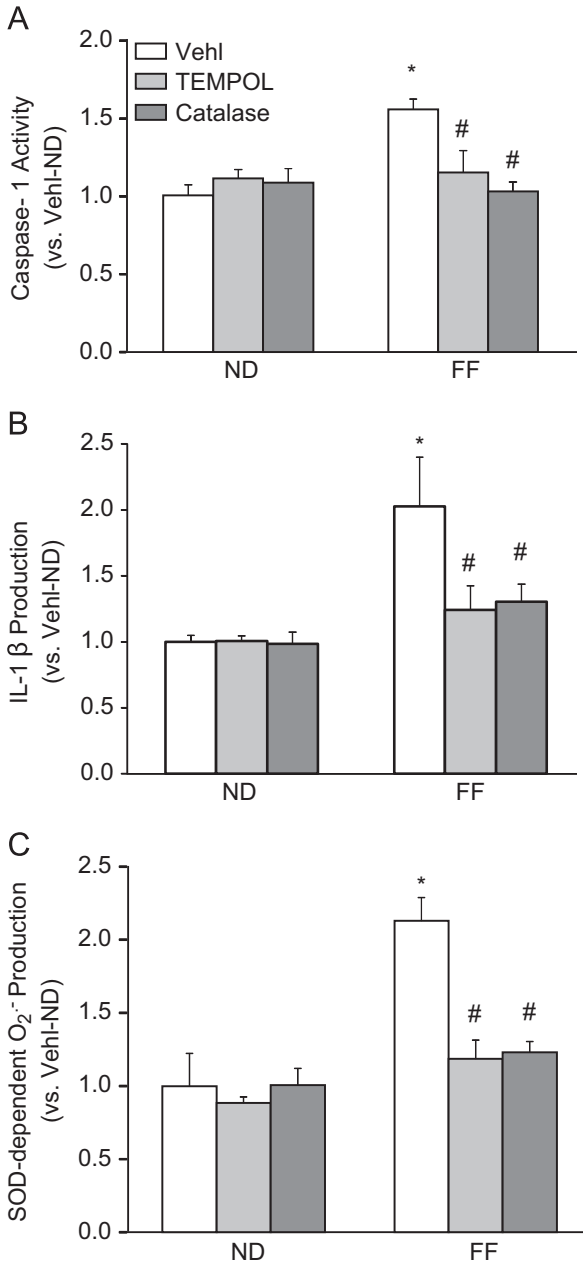

Fig. 6. In vivo administration of Tempol and catalase prevents caspase-1 activation, IL-1β production, and $O_2^{\bullet-}$ production. (A) Caspase-1 activity in Vehl-, Tempol-, or catalase-treated mice with hHcys induced by the FF diet ($n = 7$). (B) Tempol and catalase administration prevented hHcys-induced IL-1β production ($n = 6$ or 7). (C) $O_2^{\bullet-}$ production induced by hHcys was inhibited in mice treated with Tempol or catalase ($n = 6$). Vehl, vehicle; ND, normal diet; FF, folate-free diet. *$P < 0.05$ vs Vehl on ND; #$P < 0.05$ vs Vehl on FF diet.

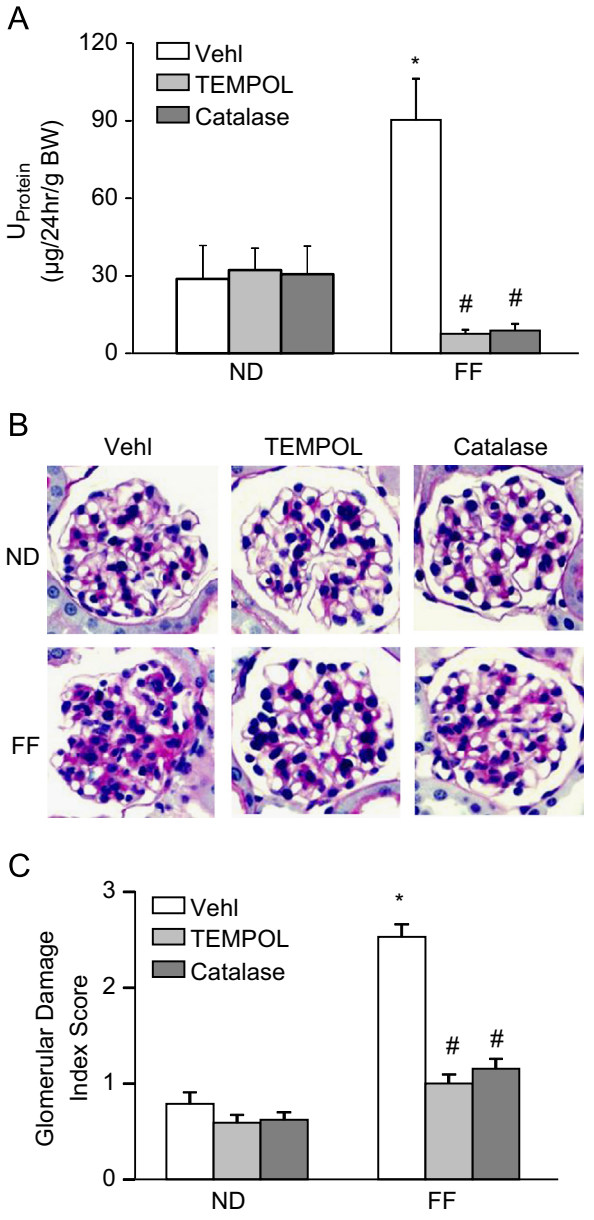

Fig. 7. Renal protective effects of $O_2^{\bullet-}$ and H_2O_2 inhibition on hHcys-induced glomerular injury. (A) hHcys-induced proteinuria was attenuated in mice receiving Tempol or catalase treatment ($n = 6$). (B) Microscopic observation of glomeruli in PAS-stained kidney sections demonstrated that Tempol and catalase prevented hHcys-induced changes in glomerular morphological structure by preventing capillary collapse, fibrosis, cellular proliferation, and mesangial cell expansion ($n = 4$–6). (C) Extent of glomerular sclerosis was assessed semiquantitatively and expressed as the Glomerular Damage Index. Vehl, vehicle; ND, normal diet; FF, folate-free diet. *$P < 0.05$ vs Vehl on ND; #$P < 0.05$ vs Vehl on FF diet.

requirement of $O_2^{\bullet-}$ dismutation to H_2O_2 in ROS-stimulated inflammasomes, which proposes an important role for H_2O_2 not only in Hcys-induced NLRP3 inflammasome formation, but also in inflammasome formation in response to other stimuli that increase H_2O_2 production.

The $^{\bullet}OH$ scavenger TMTU did not significantly inhibit any measure of Hcys-induced NLRP3 inflammasome formation or activation, suggesting that in comparison to $O_2^{\bullet-}$ and H_2O_2, $^{\bullet}OH$ does not play a crucial role in inflammasome stimulation. Although TMTU did not produce inhibitory effects that were of statistical significance, caspase-1 activity and IL-1β production appeared lower when TMTU was used. This effect may be due to some nonspecific action of TMTU because thiourea compounds, although commonly used as potent scavengers of $^{\bullet}OH$, are also able to scavenge $O_2^{\bullet-}$ and H_2O_2 at higher doses [58,59].

An important role for $ONOO^-$ in many disease processes is supported throughout the literature, including Hcys-induced cardiovascular and renal injury, in which $ONOO^-$ participates in detrimental events such as endothelial dysfunction and renal ischemia–reperfusion injury [60–65]. Therefore, we examined the role of $ONOO^-$ scavenging on Hcys-induced NLRP3 inflammasome formation and activation in podocytes. It was found that ebselen, a putative $ONOO^-$ scavenger, failed to decrease formation and activation of NLRP3 inflammasomes in podocytes treated with Hcys, suggesting $ONOO^-$ may not play a critical redox role in this particular pathological process in podocytes.

With respect to the models of NLRP3 inflammasome activation, there is debate whether pro- or antioxidant events contribute to this phenomenon. Our study, along with many of the aforementioned studies, provided supportive evidence for a ROS-dependent mechanism that can be hindered when these species are scavenged. This concept, however, has been challenged, with evidence demonstrating that ROS inhibition prevents the priming, but not activation, of inflammasomes [66]. Furthermore, monocytes and macrophages isolated from patients with chronic granulomatous disease and from NADPH oxidase-deficient mice exhibited typical IL-1β secretion [67,68], which was different from our results in podocytes [14]. It is possible that different cell types may have altered sensitivity to redox regulation of NLRP3 inflammasomes or to different danger signals. Activation of NLRP3 or other inflammasomes in macrophages in vitro may require a priming process, a step that perhaps is not necessary in other cell types [13,69]. In addition, because NLRP3 inflammasome activation requires only a low level of intracellular $O_2^{\bullet -}$ or H_2O_2 as a signaling mechanism rather than a injurious event, monocytes and macrophages isolated from patients with chronic granulomatous disease and from NADPH oxidase-deficient mice may still have enough ROS to stimulate NLRP3 inflammasome activation and IL-1β production. Other ROS-producing pathways in these sick cells may also exert compensatory redox regulation to NLRP3 inflammasome activation. Additional studies are needed to further explore such potential for the redox regulation of NLRP3 inflammasomes in different cell types.

In summary, this study demonstrated that reducing $O_2^{\bullet -}$ and H_2O_2 inhibited NLRP3 inflammasome formation and consequent processing of IL-1β, suggesting that both species are importantly implicated in the instigation of Hcys-induced NLRP3 inflammasome activation in cultured podocytes. Similar effects were seen in vivo in glomerular podocytes of hyperhomocysteinemic mice, in which dismutation of $O_2^{\bullet -}$ by Tempol and decomposition of H_2O_2 by catalase not only prevented glomerular NLRP3 inflammasome formation and activation, but also importantly protected against hHcys-induced glomerular injury and dysfunction. Together, these results indicate that $O_2^{\bullet -}$ and H_2O_2 contribute to inflammasome triggering, podocyte injury, and potential progression to glomerular sclerosis and end-stage renal disease during hHcys.

Acknowledgment

This work was supported by Grants DK54927, HL075316, and HL57244 (to P.L.) and 1F31AG043289-01 (to J.M.A.) from the National Institutes of Health.

Appendix A. Supplementary material

Supplementary data associated with this article can be found in the online version at http://dx.doi.org/10.1016/j.freeradbiomed.2013.10.009.

References

[1] Perla-Kajan, J.; Jakubowski, H. Paraoxonase 1 and homocysteine metabolism. *Amino Acids* **43:**1405–1417; 2012.
[2] Cavalca, V.; Cighetti, G.; Bamonti, F.; Loaldi, A.; Bortone, L.; Novembrino, C.; De Franceschi, M.; Belardinelli, R.; Guazzi, M. D. Oxidative stress and homocysteine in coronary artery disease. *Clin Chem* **47:**887–892; 2001.
[3] Bialecka, M.; Kurzawski, M.; Roszmann, A.; Robowski, P.; Sitek, E. J.; Honczarenko, K.; Gorzkowska, A.; Budrewicz, S.; Mak, M.; Jarosz, M.; Golab-Janowska, M.; Koziorowska-Gawron, E.; Drozdzik, M.; Slawek, J. Association of COMT, MTHFR, and SLC19A1(RFC-1) polymorphisms with homocysteine blood levels and cognitive impairment in Parkinson's disease. *Pharmacogenet Genomics* **22:**716–724; 2012.
[4] Schalinske, K. L.; Smazal, A. L. Homocysteine imbalance: a pathological metabolic marker. *Adv Nutr* **3:**755–762; 2012.
[5] Yu, M.; Sturgill-Short, G.; Ganapathy, P.; Tawfik, A.; Peachey, N. S.; Smith, S. B. Age-related changes in visual function in cystathionine-beta-synthase mutant mice, a model of hyperhomocysteinemia. *Exp Eye Res* **96:**124–131; 2012.
[6] McLean, R. R.; Jacques, P. F.; Selhub, J.; Tucker, K. L.; Samelson, E. J.; Broe, K. E.; Hannan, M. T.; Cupples, L. A.; Kiel, D. P. Homocysteine as a predictive factor for hip fracture in older persons. *N Engl J Med* **350:**2042–2049; 2004.
[7] Schafer, S. A.; Mussig, K.; Stefan, N.; Haring, H. U.; Fritsche, A.; Balletshofer, B. M. Plasma homocysteine concentrations in young individuals at increased risk of type 2 diabetes are associated with subtle differences in glomerular filtration rate but not with insulin resistance. *Exp Clin Endocrinol Diabetes* **114:**306–309; 2006.
[8] Hwang, S. Y.; Siow, Y. L.; Au-Yeung, K. K.; House, J.; O, K. Folic acid supplementation inhibits NADPH oxidase-mediated superoxide anion production in the kidney. *Am J Physiol Renal Physiol* **300:**F189–F198; 2011.
[9] Wu, C. C.; Zheng, C. M.; Lin, Y. F.; Lo, L.; Liao, M. T.; Lu, K. C. Role of homocysteine in end-stage renal disease. *Clin Biochem* **45:**1286–1294; 2012.
[10] Zhang, C.; Yi, F.; Xia, M.; Boini, K. M.; Zhu, Q.; Laperle, L. A.; Abais, J. M.; Brimson, C. A.; Li, P. L. NMDA receptor-mediated activation of NADPH oxidase and glomerulosclerosis in hyperhomocysteinemic rats. *Antioxid Redox Signal* **13:**975–986; 2010.
[11] Yi, F.; Xia, M.; Li, N.; Zhang, C.; Tang, L.; Li, P. L. Contribution of guanine nucleotide exchange factor Vav2 to hyperhomocysteinemic glomerulosclerosis in rats. *Hypertension* **53:**90–96; 2009.
[12] Yi, F.; Chen, Q. Z.; Jin, S.; Li, P. L. Mechanism of homocysteine-induced Rac1/NADPH oxidase activation in mesangial cells: role of guanine nucleotide exchange factor Vav2. *Cell Physiol Biochem* **20:**909–918; 2007.
[13] Zhang, C.; Boini, K. M.; Xia, M.; Abais, J. M.; Li, X.; Liu, Q.; Li, P. L. Activation of Nod-like receptor protein 3 inflammasomes turns on podocyte injury and glomerular sclerosis in hyperhomocysteinemia. *Hypertension* **60:**154–162; 2012.
[14] Abais, J. M.; Zhang, C.; Xia, M.; Liu, Q.; Gehr, T. W.; Boini, K. M.; Li, P. L. NADPH Oxidase-Mediated Triggering of Inflammasome Activation in Mouse Podocytes and Glomeruli During Hyperhomocysteinemia. *Antioxid Redox Signal*; 2012.
[15] Lambeth, J. D. Nox enzymes, ROS, and chronic disease: an example of antagonistic pleiotropy. *Free Radic Biol Med* **43:**332–347; 2007.
[16] Dostert, C.; Petrilli, V.; Van Bruggen, R.; Steele, C.; Mossman, B. T.; Tschopp, J. Innate immune activation through Nalp3 inflammasome sensing of asbestos and silica. *Science* **320:**674–677; 2008.
[17] Martinon, F.; Petrilli, V.; Mayor, A.; Tardivel, A.; Tschopp, J. Gout-associated uric acid crystals activate the NALP3 inflammasome. *Nature* **440:**237–241; 2006.
[18] Watanabe, H.; Gaide, O.; Petrilli, V.; Martinon, F.; Contassot, E.; Roques, S.; Kummer, J. A.; Tschopp, J.; French, L. E. Activation of the IL-1beta-processing inflammasome is involved in contact hypersensitivity. *J Invest Dermatol* **127:**1956–1963; 2007.
[19] Zhou, R.; Tardivel, A.; Thorens, B.; Choi, I.; Tschopp, J. Thioredoxin-interacting protein links oxidative stress to inflammasome activation. *Nat Immunol* **11:**136–140; 2010.
[20] Nishi, Y.; Satoh, M.; Nagasu, H.; Kadoya, H.; Ihoriya, C.; Kidokoro, K.; Sasaki, T.; Kashihara, N. Selective estrogen receptor modulation attenuates proteinuria-induced renal tubular damage by modulating mitochondrial oxidative status. *Kidney Int* **83:**662–673; 2013.
[21] Wang, C.; Pan, Y.; Zhang, Q. Y.; Wang, F. M.; Kong, L. D. Quercetin and allopurinol ameliorate kidney injury in STZ-treated rats with regulation of renal NLRP3 inflammasome activation and lipid accumulation. *PLoS One* **7:**e38285; 2012.
[22] Wang, W.; Wang, X.; Chun, J.; Vilaysane, A.; Clark, S.; French, G.; Bracey, N. A.; Trpkov, K.; Bonni, S.; Duff, H. J.; Beck, P. L.; Muruve, D. A. Inflammasome-independent NLRP3 augments TGF-beta signaling in kidney epithelium. *J Immunol* **190:**1239–1249; 2013.
[23] Yin, Y.; Yan, Y.; Jiang, X.; Mai, J.; Chen, N. C.; Wang, H.; Yang, X. F. Inflammasomes are differentially expressed in cardiovascular and other tissues. *Int J Immunopathol Pharmacol* **22:**311–322; 2009.
[24] Yin, Y.; Pastrana, J. L.; Li, X.; Huang, X.; Mallilankaraman, K.; Choi, E. T.; Madesh, M.; Wang, H.; Yang, X. F. Inflammasomes: sensors of metabolic stresses for vascular inflammation. *Front Biosci (Landmark Ed)* **18:**638–649; 2013.
[25] Jin, C.; Flavell, R. A. Inflammasome activation. The missing link: how the inflammasome senses oxidative stress. *Immunol Cell Biol* **88:**510–512; 2010.
[26] Tschopp, J.; Schroder, K. NLRP3 inflammasome activation: The convergence of multiple signalling pathways on ROS production? *Nat Rev Immunol* **10:**210–215; 2010.
[27] Gross, O.; Thomas, C. J.; Guarda, G.; Tschopp, J. The inflammasome: an integrated view. *Immunol Rev* **243:**136–151; 2011.
[28] Zhang, C.; Hu, J. J.; Xia, M.; Boini, K. M.; Brimson, C. A.; Laperle, L. A.; Li, P. L. Protection of podocytes from hyperhomocysteinemia-induced injury by deletion of the gp91phox gene. *Free Radic Biol Med* **48:**1109–1117; 2010.
[29] Yi, F.; Zhang, A. Y.; Li, N.; Muh, R. W.; Fillet, M.; Renert, A. F.; Li, P. L. Inhibition of ceramide-redox signaling pathway blocks glomerular injury in hyperhomocysteinemic rats. *Kidney Int* **70:**88–96; 2006.
[30] Joles, J. A.; Kunter, U.; Janssen, U.; Kriz, W.; Rabelink, T. J.; Koomans, H. A.; Floege, J. Early mechanisms of renal injury in hypercholesterolemic or hypertriglyceridemic rats. *J Am Soc Nephrol* **11:**669–683; 2000.

[31] Neuman, J. C.; Albright, K. A.; Schalinske, K. L. Exercise prevents hyperhomocysteinemia in a dietary folate-restricted mouse model. *Nutr Res* **33:**487–493; 2013.
[32] Nishiyama, A.; Yoshizumi, M.; Hitomi, H.; Kagami, S.; Kondo, S.; Miyatake, A.; Fukunaga, M.; Tamaki, T.; Kiyomoto, H.; Kohno, M.; Shokoji, T.; Kimura, S.; Abe, Y. The SOD mimetic tempol ameliorates glomerular injury and reduces mitogen-activated protein kinase activity in Dahl salt-sensitive rats. *J Am Soc Nephrol* **15:**306–315; 2004.
[33] Sousa, T.; Oliveira, S.; Afonso, J.; Morato, M.; Patinha, D.; Fraga, S.; Carvalho, F.; Albino-Teixeira, A. Role of H(2)O(2) in hypertension, renin-angiotensin system activation and renal medullary disfunction caused by angiotensin II. *Br J Pharmacol* **166:**2386–2401; 2012.
[34] Boini, K. M.; Xia, M.; Xiong, J.; Li, C.; Payne, L. P.; Li, P. L. Implication of CD38 gene in podocyte epithelial-to-mesenchymal transition and glomerular sclerosis. *J Cell Mol Med* **16:**1674–1685; 2012.
[35] Abulafia, D. P.; de Rivero Vaccari, J. P.; Lozano, J. D.; Lotocki, G.; Keane, R. W.; Dietrich, W. D. Inhibition of the inflammasome complex reduces the inflammatory response after thromboembolic stroke in mice. *J Cereb Blood Flow Metab* **29:**534–544; 2009.
[36] Boini, K. M.; Xia, M.; Li, C.; Zhang, C.; Payne, L. P.; Abais, J. M.; Poklis, J. L.; Hylemon, P. B.; Li, P. L. Acid sphingomyelinase gene deficiency ameliorates the hyperhomocysteinemia-induced glomerular injury in mice. *Am J Pathol* **179:**2210–2219; 2011.
[37] Xu, M.; Zhang, Y.; Xia, M.; Li, X. X.; Ritter, J. K.; Zhang, F.; Li, P. L. NAD(P)H oxidase-dependent intracellular and extracellular O2*- production in coronary arterial myocytes from CD38 knockout mice. *Free Radic Biol Med* **52:**357–365; 2012.
[38] Zhang, C.; Xia, M.; Boini, K. M.; Li, C. X.; Abais, J. M.; Li, X. X.; Laperle, L. A.; Li, P. L. Epithelial-to-mesenchymal transition in podocytes mediated by activation of NADPH oxidase in hyperhomocysteinemia. *Pflugers Arch* **462:**455–467; 2011.
[39] Narayan, S. K.; Saxby, B. K.; Firbank, M. J.; O'Brien, J. T.; Harrington, F.; McKeith, I. G.; Hansrani, M.; Stansby, G.; Ford, G. A. Plasma homocysteine and cognitive decline in older hypertensive subjects. *Int Psychogeriatr* **23:**1607–1615; 2011.
[40] Badiou, S.; Dupuy, A. M.; Jaussent, I.; Sultan, A.; Mariano-Goulart, D.; Cristol, J. P.; Avignon, A. Homocysteine as a determinant of left ventricular ejection fraction in patients with diabetes. *Clin Chem Lab Med* **50:**1099–1106; 2012.
[41] Vasan, R. S.; Beiser, A.; D'Agostino, R. B.; Levy, D.; Selhub, J.; Jacques, P. F.; Rosenberg, I. H.; Wilson, P. W. Plasma homocysteine and risk for congestive heart failure in adults without prior myocardial infarction. *JAMA* **289:**1251–1257; 2003.
[42] Valentino, F.; Bivona, G.; Butera, D.; Paladino, P.; Fazzari, M.; Piccoli, T.; Ciaccio, M.; La Bella, V. Elevated cerebrospinal fluid and plasma homocysteine levels in ALS. *Eur J Neurol* **17:**84–89; 2010.
[43] Levin, J.; Botzel, K.; Giese, A.; Vogeser, M.; Lorenzl, S. Elevated levels of methylmalonate and homocysteine in Parkinson's disease, progressive supranuclear palsy and amyotrophic lateral sclerosis. *Dement Geriatr Cogn Disord* **29:**553–559; 2010.
[44] Yi, F.; Li, P. L. Mechanisms of homocysteine-induced glomerular injury and sclerosis. *Am J Nephrol* **28:**254–264; 2008.
[45] Liao, P. C.; Chao, L. K.; Chou, J. C.; Dong, W. C.; Lin, C. N.; Lin, C. Y.; Chen, A.; Ka, S. M.; Ho, C. L.; Hua, K. F. Lipopolysaccharide/adenosine triphosphate-mediated signal transduction in the regulation of NLRP3 protein expression and caspase-1-mediated interleukin-1beta secretion. *Inflamm Res* **62:**89–96; 2013.
[46] Varga, A.; Budai, M. M.; Milesz, S.; Bacsi, A.; Tozser, J.; Benko, S. Ragweed pollen extract intensifies lipopolysaccharide-induced priming of NLRP3 inflammasome in human macrophages. *Immunology* **138:**392–401; 2013.
[47] Cassel, S. L.; Eisenbarth, S. C.; Iyer, S. S.; Sadler, J. J.; Colegio, O. R.; Tephly, L. A.; Carter, A. B.; Rothman, P. B.; Flavell, R. A.; Sutterwala, F. S. The Nalp3 inflammasome is essential for the development of silicosis. *Proc Natl Acad Sci U S A* **105:**9035–9040; 2008.
[48] Cruz, C. M.; Rinna, A.; Forman, H. J.; Ventura, A. L.; Persechini, P. M.; Ojcius, D. M. ATP activates a reactive oxygen species-dependent oxidative stress response and secretion of proinflammatory cytokines in macrophages. *J Biol Chem* **282:**2871–2879; 2007.
[49] Pelegrin, P.; Surprenant, A. Dynamics of macrophage polarization reveal new mechanism to inhibit IL-1beta release through pyrophosphates. *EMBO J* **28:**2114–2127; 2009.
[50] Lindauer, M.; Wong, J.; Magun, B. Ricin Toxin Activates the NALP3 Inflammasome. *Toxins (Basel)* **2:**1500–1514; 2010.
[51] Tojo, A.; Asaba, K.; Onozato, M. L. Suppressing renal NADPH oxidase to treat diabetic nephropathy. *Expert Opin Ther Targets* **11:**1011–1018; 2007.
[52] Wilcox, C. S. Effects of tempol and redox-cycling nitroxides in models of oxidative stress. *Pharmacol Ther* **126:**119–145; 2010.
[53] Peixoto, E. B.; Papadimitriou, A.; Lopes de Faria, J. M.; Lopes de Faria, J. B. Tempol reduces podocyte apoptosis via PARP signaling pathway in experimental diabetes mellitus. *Nephron Exp Nephrol* **120:**e81–e90; 2012.
[54] Yang, Z. Z.; Zhang, A. Y.; Yi, F. X.; Li, P. L.; Zou, A. P. Redox regulation of HIF-1alpha levels and HO-1 expression in renal medullary interstitial cells. *Am J Physiol Renal Physiol* **284:**F1207–F1215; 2003.
[55] Beaman, M.; Birtwistle, R.; Howie, A. J.; Michael, J.; Adu, D. The role of superoxide anion and hydrogen peroxide in glomerular injury induced by puromycin aminonucleoside in rats. *Clin Sci (Lond)* **73:**329–332; 1987.
[56] Birtwistle, R. J.; Michael, J.; Howie, A. J.; Adu, D. Reactive oxygen products in heterologous anti-glomerular basement membrane nephritis in rats. *Br J Exp Pathol* **70:**207–213; 1989.
[57] Villegas, L. R.; Kluck, D.; Field, C.; Oberley-Deegan, R. E.; Woods, C.; Yeager, M. E.; El Kasmi, K. C.; Savani, R. C.; Bowler, R. P.; Nozik-Grayck, E. Superoxide Dismutase Mimetic, MnTE-2-PyP, Attenuates Chronic Hypoxia-Induced Pulmonary Hypertension, Pulmonary Vascular Remodeling, and Activation of the NALP3 Inflammasome. *Antioxid Redox Signal* ; 2013.
[58] Kelner, M. J.; Bagnell, R.; Welch, K. J. Thioureas react with superoxide radicals to yield a sulfhydryl compound. Explanation for protective effect against paraquat. *J Biol Chem* **265:**1306–1311; 1990.
[59] Wasil, M.; Halliwell, B.; Grootveld, M.; Moorhouse, C. P.; Hutchison, D. C.; Baum, H. The specificity of thiourea, dimethylthiourea and dimethyl sulphoxide as scavengers of hydroxyl radicals. Their protection of alpha 1-antiproteinase against inactivation by hypochlorous acid. *Biochem J* **243:**867–870; 1987.
[60] Cheng, Z.; Jiang, X.; Kruger, W. D.; Pratico, D.; Gupta, S.; Mallilankaraman, K.; Madesh, M.; Schafer, A. I.; Durante, W.; Yang, X.; Wang, H. Hyperhomocysteinemia impairs endothelium-derived hyperpolarizing factor-mediated vasorelaxation in transgenic cystathionine beta synthase-deficient mice. *Blood* **118:**1998–2006; 2011.
[61] Prathapasinghe, G. A.; Siow, Y. L. O, K. Detrimental role of homocysteine in renal ischemia-reperfusion injury. *Am J Physiol Renal Physiol* **292:**F1354–F1363; 2007.
[62] Sibinga, N. E. Channeling the homocysteine chapel. *Blood* **118:**1717–1719; 2011.
[63] Vacek, T. P.; Qipshidze, N.; Tyagi, S. C. Hydrogen sulfide and sodium nitroprusside compete to activate/deactivate MMPs in bone tissue homogenates. *Vasc Health Risk Manag* **9:**117–123; 2013.
[64] Levrand, S.; Pacher, P.; Pesse, B.; Rolli, J.; Feihl, F.; Waeber, B.; Liaudet, L. Homocysteine induces cell death in H9C2 cardiomyocytes through the generation of peroxynitrite. *Biochem Biophys Res Commun* **359:**445–450; 2007.
[65] Rosenberger, D.; Moshal, K. S.; Kartha, G. K.; Tyagi, N.; Sen, U.; Lominadze, D.; Maldonado, C.; Roberts, A. M.; Tyagi, S. C. Arrhythmia and neuronal/endothelial myocyte uncoupling in hyperhomocysteinemia. *Arch Physiol Biochem* **112:**219–227; 2006.
[66] Bauernfeind, F.; Bartok, E.; Rieger, A.; Franchi, L.; Nunez, G.; Hornung, V. Cutting edge: reactive oxygen species inhibitors block priming, but not activation, of the NLRP3 inflammasome. *J Immunol* **187:**613–617; 2011.
[67] Hornung, V.; Bauernfeind, F.; Halle, A.; Samstad, E. O.; Kono, H.; Rock, K. L.; Fitzgerald, K. A.; Latz, E. Silica crystals and aluminum salts activate the NALP3 inflammasome through phagosomal destabilization. *Nat Immunol* **9:**847–856; 2008.
[68] van Bruggen, R.; Koker, M. Y.; Jansen, M.; van Houdt, M.; Roos, D.; Kuijpers, T. W.; van den Berg, T. K. Human NLRP3 inflammasome activation is Nox1-4 independent. *Blood* **115:**5398–5400; 2010.
[69] Savage, C. D.; Lopez-Castejon, G.; Denes, A.; Brough, D. NLRP3-Inflammasome Activating DAMPs Stimulate an Inflammatory Response in Glia in the Absence of Priming Which Contributes to Brain Inflammation after Injury. *Front Immunol* **3:**288; 2012.